Large Cage Face-Centered-Cubic *Fm*3*m* Mesoporous Silica: Synthesis and Structure

Freddy Kleitz,[†] Dinan Liu,[†] Gopinathan M. Anilkumar,[†] In-Soo Park,[†] Leonid A. Solovyov,[‡] Alexandr N. Shmakov,[§] and Ryong Ryoo*[,†]

National Creative Research Initiative Center for Functional Nanomaterials, Department of Chemistry (School of Molecular Science-BK21), Korea Advanced Institute of Science and Technology, Daejeon, 305-701, Republic of Korea, Institute of Chemistry and Chemical Technology, 660049 Krasnoyarsk, Russia, and Boreskov Institute of Catalysis, 630090 Novosibirsk, Russia

Received: July 22, 2003; In Final Form: October 14, 2003

The synthesis and precise structural characterization of highly ordered three-dimensional close-packed cage-type mesoporous silica is reported. The siliceous mesoporous material is proven to be commensurate with the face-centered-cubic *Fm*3*m* symmetry in high purity by a combination of experimental and simulated powder X-ray diffraction (XRD) and transmission electron microscopy (TEM) analyses. The cage-type calcined samples were additionally characterized by nitrogen physisorption. The aqueous synthesis method to prepare large cage mesoporous silica with cubic *Fm*3*m* structure is based on the use of $EO_{106}PO_{70}EO_{106}$ triblock copolymer (F127) at low HCl concentrations, with no additional salts or organic additives. Here, emphasis is put on the low HCl concentration regime, allowing the facile thermodynamic control of the silica−triblock copolymer mesophase self-assembly. Further, simple application of hydrothermal treatments at various temperatures ranging from 45 to 150 °C enables the tailoring of the mesopore diameters and apertures. The combination of experimental and simulated XRD patterns and TEM images is confirmed to be a very powerful means for the accurate elucidation of the structure of new mesoporous materials.

Introduction

The recent discovery of ordered mesoporous materials has opened prospects for the development of new technologies in catalysis, separation, drug delivery, and nanoscience, owing to their tunable size nanopores, high surface areas, versatile possibilities of surface functionalization, and diversity in composition, structure, and morphology.[1] Of particular current interest are mesoporous silicas consisting of interconnected large cage-type pores (pore diameter > 5 nm) being organized in a three-dimensional (3-D) network. For instance, large pore cage-type mesoporous silica designated as SBA-16,[2] synthesized in acidic media with poly(ethylene oxide)−poly(propylene oxide)−poly(ethylene oxide) triblock copolymers ($EO_nPO_mEO_n$ for brevity) and tetraethoxysilane (TEOS) as the silica source, consists of spherical cavities of 9−10 nm in diameter arranged in a body-centered-cubic array (with *Im*3*m* symmetry), and connected through a mesoporous opening of 2.0−2.5 nm.[3] Such types of highly interconnected 3-D mesostructured porous materials are expected to be superior to hexagonal structures with one-dimensional channels, especially for applications involving selectively tuned diffusion, immobilization of large molecules, or host−guest interactions within nanostructured materials. Furthermore, materials such as two-dimensional hexagonal SBA-15 mesoporous silica[2] are available to be used as model systems for adsorption behavior and diffusion studies in cylindrical pores, while there is still a need for ideal model systems of close-packed spherical cavities.

Although numerous reports have dealt with the preparation of large pore ordered mesoporous silicas,[2−11] the ability to control synthesis conditions providing efficient tuning of the structural and textural properties is still rather limited, with often an uncertain degree of ordering and phase purity. With respect to this, the synthesis of pure phase large pore 3-D mesoporous silica, with high quality, still remains challenging. A large cage-type mesoporous silica designated as FDU-1,[6] first reported to have body-centered-cubic *Im*3*m* symmetry, was more recently shown by other authors to exhibit face-centered-cubic *Fm*3*m* structure with, however, clear evidence of intergrowths with 3-D hexagonal phase.[9] Previous efforts by Sakamoto et al.[12] led to the preparation of a phase-pure cubic *Fm*3*m* mesoporous structure that was, however, an organofunctionalized silica rather than a pure silica material, and showed relatively small pore diameter (<4−5 nm). Only very recently, while the present paper was in preparation, a synthesis method presumably leading to another large cagelike mesoporous silica was proposed by Fan et al.[13] This rather complicated synthesis uses a triblock copolymer and TEOS in the presence of a salt (KCl) and an organic additive (trimethylbenzene), with a high concentration of hydrochloric acid and extensive reaction time under hydrothermal conditions (72 h). These authors have suggested that the cagelike mesoporous siliceous material has cubic symmetry with *Fm*3*m* space group. However, they did not demonstrate evidently that it was a cubic close packing of spherical cavities with *Fm*3*m* symmetry, as judged by their oversimplified structural assignment. Particularly, the X-ray powder diffraction (XRD) patterns presented in ref 13 did not resolve the (111) and (200) reflections expected for face-centered close-packed structures. Also, the indexing of the sequence of diffraction peaks cannot be used as a direct criterion for symmetry assignment since the same sequence can be indexed in different ways, including *Fm*3*m*, *Ia*3*d* (with $\sqrt{2}$ bigger unit cell), and several 3-D hexagonal or rhombohedral variants of the lattice.

* To whom correspondence should be addressed. Fax: (+82) 42 869 8130. E-mail: rryoo@kaist.ac.kr.
[†] Korea Advanced Institute of Science and Technology.
[‡] Institute of Chemistry and Chemical Technology.
[§] Boreskov Institute of Catalysis.

10.1021/jp036136b CCC: $25.00
Published on Web 12/02/2003

Further, the transmission electron microscopy (TEM) investigations performed by Fan et al. did not give a definite assignment either, and the absence of the hexagonal intergrowths was stated but not substantiated.

Herein, we describe a straightforward synthesis route to highly ordered 3-D close-packed cage-type mesoporous silica, with the emphasis on the low HCl concentration regime in aqueous solution allowing facile thermodynamic control of the silica mesophase formation. The new material is proven to be commensurate with 3-D close-packed cage-type *Fm*3*m* cubic mesostructure in high purity. Regarding this, we demonstrate that the combination of experimental and simulated X-ray diffraction patterns and TEM images ensures the required detailed and accurate elucidation of the structure.

Experimental Section

Materials. The large mesopore *Fm*3*m* silica, designated as KIT-5 for brevity, was prepared in aqueous solution using EO_{106}-$PO_{70}EO_{106}$ (Pluronic F127, Sigma) as a structure-directing agent, and TEOS as the silica precursor (ACROS, 98%). High-quality samples were obtained with low HCl concentrations of 0.4−0.5 M. In a typical synthesis, 5.00 g of F127 was dissolved in 240 g of distilled water and 10.5 g of concentrated hydrochloric acid (35 wt % HCl). To this mixture, 24.0 g of TEOS was quickly added under stirring at 45 °C. The mixture was stirred at 45 °C for 24 h for the formation of the mesostructured product. Subsequently, the reaction mixture was heated for 24 h at 100 °C under static conditions for hydrothermal treatment. The solid product was then filtered and dried at 100 °C without washing. The molar composition of the reaction mixture TEOS/F127/HCl/H_2O was 1.00/0.0035/0.88/119. To remove the template, the solid was briefly slurried in an ethanol/HCl mixture, filtered, dried, and then calcined in air flow at 550 °C. In another set of experiments, the hydrothermal treatment temperature, under static conditions following the initial reaction at 45 °C, was varied from 45 to 150 °C. As-synthesized samples and samples calcined at 550 °C are referred to as AS-*T* and CA-*T*, respectively, with *T* denoting the reaction temperature. The hydrothermal treatment time was given as 24 h unless specified otherwise in parentheses following *T*.

Measurements. The N_2 adsorption−desorption isotherms were obtained on a Quantachrome Autosorb-1MP instrument at 77 K. All samples were outgassed at 300 °C for 6 h prior to the measurements. The XRD powder patterns were measured on a Rigaku Multiplex diffractometer operated at 2 kW, using Cu Kα radiation, in the range of 0.55°−3.0° (2θ) with a step width 0.01° (2θ) and count time of 5.0 s. Synchrotron XRD data were collected on a high-resolution diffractometer located in the Siberian Center of Synchrotron Radiation. A Ge(111) plane perfect crystal analyzer on the diffracted beam ($\lambda = 0.154$ nm) along with a high natural collimation of the synchrotron beam provided high instrumental resolution of the diffractometer. For TEM observation, calcined samples were dispersed in ethanol (99.9 vol %) using the ultrasonic method, and the suspension was subsequently dropped onto a carbon microgrid. The transmission electron microscopy observations were performed on a Phillips F20 Tecnai instrument, operated at 160 kV.

Methods. XRD structure modeling was performed using the continuous density function (CDF) approach.[14] The averaged density distribution in the materials was simulated by a flexible analytical continuous function having adjustable parameters. The intensities of the diffraction reflections were calculated using the Fourier transform of the model function. The internal structure disorder was allowed for by incorporating the Debye−Waller factor. The Rietveld full-profile formalism[15] was used for XRD powder profile calculations. The TEM simulations were performed by projecting the density distribution function obtained from the CDF modeling onto respective crystallographic planes.

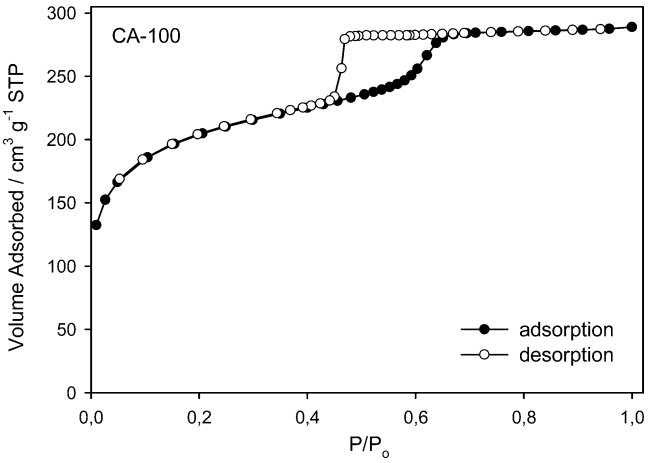

Figure 1. Nitrogen physisorption isotherm at 77 K obtained for cubic KIT-5 mesoporous silica synthesized at 100 °C (CA-100).

TABLE 1: Structural Properties of the Samples Synthesized at 45 and 100 °C

samples	unit cell *a* [nm]	cage diam w_{XRD} [nm]	cage diam w_{MSC}[a] [nm]	surf area S_{BET}[b] [m^2 g^{-1}]	pore vol[c] [cm^3 g^{-1}]
AS-45	20.5	6.8			
CA-45	17.0	6.4	6.8	390	0.21
AS-100	21.7	8.3			
CA-100	19.0	8.3	9.3	715	0.45

[a] Model of spherical cavities described in detail in refs 10a and 8 used for a face-centered-cubic structure with the unit cell determined by XRD. Micro- and mesopore volumes were evaluated using the *t*-plot method. [b] BET method. [c] Total pore volume.

Results and Discussion

The nitrogen adsorption−desorption isotherm obtained for calcined mesoporous KIT-5 silica is a type IV (Figure 1) with a sharp capillary condensation step at high relative pressures and a broad H2 hysteresis loop that is indicative of large uniform cage-type pores.[9,16] KIT-5 typically synthesized at 100 °C (CA-100) has a BET surface area of 715 m^2 g^{-1} and total pore volume of 0.45 cm^3 g^{-1}. The conventional methods of pore size analysis assuming cylindrical pore channels, such as the BJH method,[17] were shown not to be appropriate for cage-type structures.[16] Alternatively, geometric models[9,16a] or methods based on nonlocal density functional theory (NLDFT)[16] were employed in an attempt to characterize adequately the cage dimensions. On the basis of the geometric method described by Ravikovitch et al.,[16a] the pore diameter of CA-100 was estimated to be about 9.30 nm (see Table 1). Considering the isotherm desorption branch indicating the spinodal evaporation,[9,16,18] apertures of the mesoporous cavities are regarded as being smaller than 5 nm.[16,19] In the absence of hydrothermal treatment, the material CA-45 exhibits a similar N_2 sorption isotherm characteristic of cage-type structure with, however, a less pronounced capillary condensation step attesting to much smaller mesopore volume (Figure 2). Variation of the hydrothermal treatment temperatures between 45 and 150 °C results in a progressive augmentation in nitrogen sorption capacity and mesopore volume (Figure 2). In particular, the mesopore volume

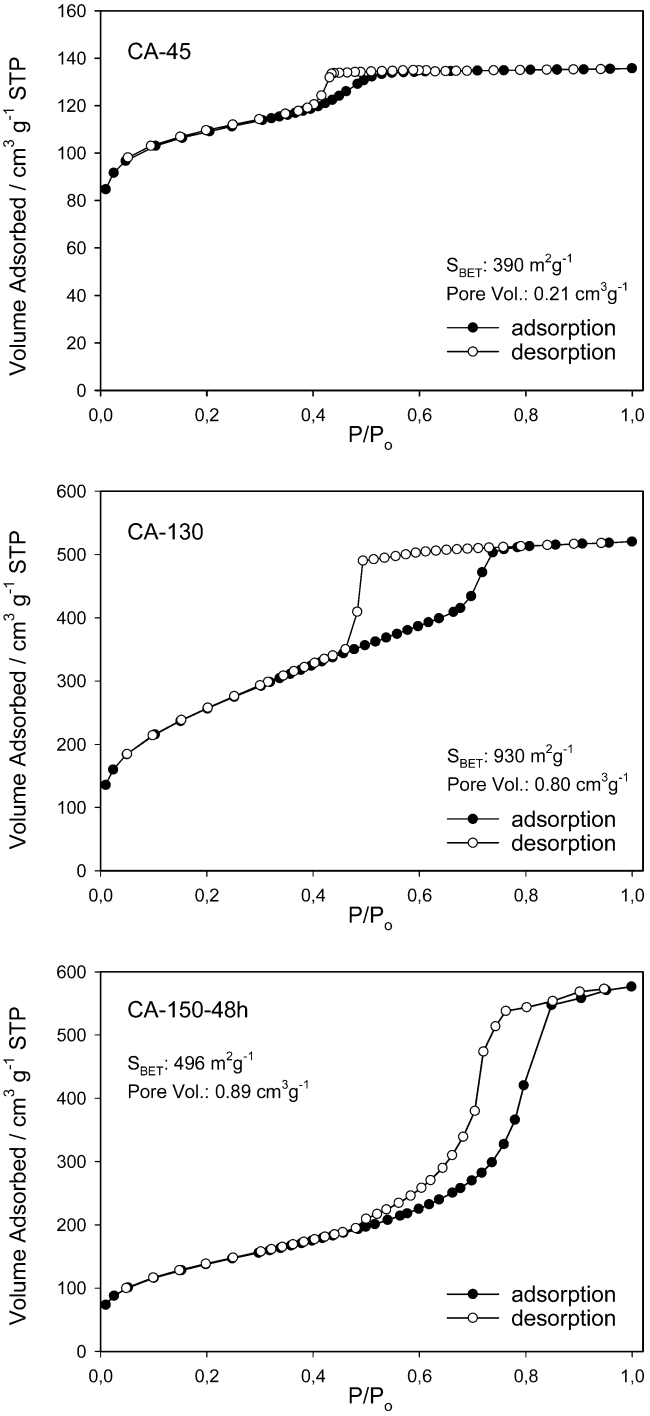

Figure 2. N_2 adsorption−desorption isotherms at 77 K for CA-45, CA-130, and CA-150(48 h).

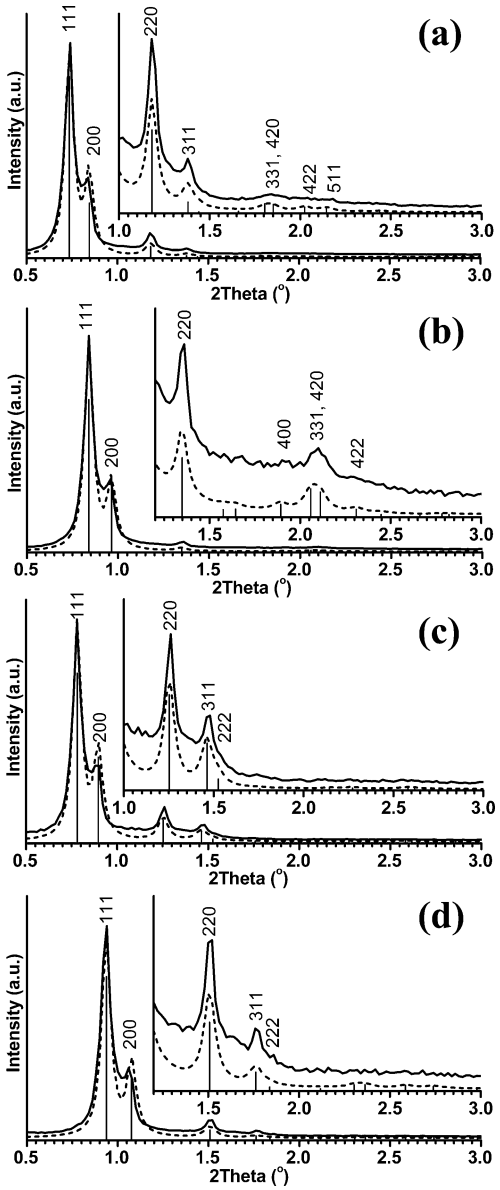

Figure 3. Experimental (solid line) and simulated (dashed line) synchrotron X-ray powder diffraction profiles obtained for cubic *Fm*3*m* KIT-5 mesoporous silica samples: (a) AS-100, (b) CA-100, (c) AS-45, and (d) CA-45. The reflection positions are marked by drop lines.

of CA-150(48 h) has been considerably increased during the prolonged hydrothermal treatment and the shape of the hysteresis loop of the N_2 isotherm suggests that pore apertures have been substantially opened. The total pore volume of this sample is 0.89 cm^3 g^{-1}. This observation agrees with previous results on FDU-1 reporting a similar transition from a cagelike structure to a more open structure as the synthesis temperature is increased.[9,19]

The lattice type and symmetry of the materials were determined by a combined analysis of TEM images and positions of the powder XRD peaks. The synchrotron XRD powder patterns are shown in Figure 3. The XRD powder patterns measured on a conventional laboratory diffractometer are added in Figure 4 (see also Supporting Information). Highly resolved low-angle diffractions are observed and can be indexed to the face-centered-cubic *Fm*3*m* symmetry lattice. No additional reflections related to the 3-D hexagonal intergrowths are observed. To verify this symmetry assignment, the XRD and TEM structure modeling was performed using the CDF approach. Since the physisorption analysis pointed to the cage-type structure of the materials, the density distribution was simulated by a three-dimensional array of spherical cavities. The centers of cavities were located in 4a Wyckoff positions of the cubic *Fm*3*m* lattice, namely (0,0,0), (0,1/2,1/2), (1/2,1/2,0), and (1/2,0,1/2), in accordance with the close-packing principle. The value of the continuous density function between the cavities was set to a constant value, simulating the averaged density distribution of amorphous silica in the walls. The interconnections between the cavities were not included in the structure model, since at this stage of study we focused only on a qualitative characterization. The cavity diameter and the cubic lattice parameter were varied to obtain the best agreement

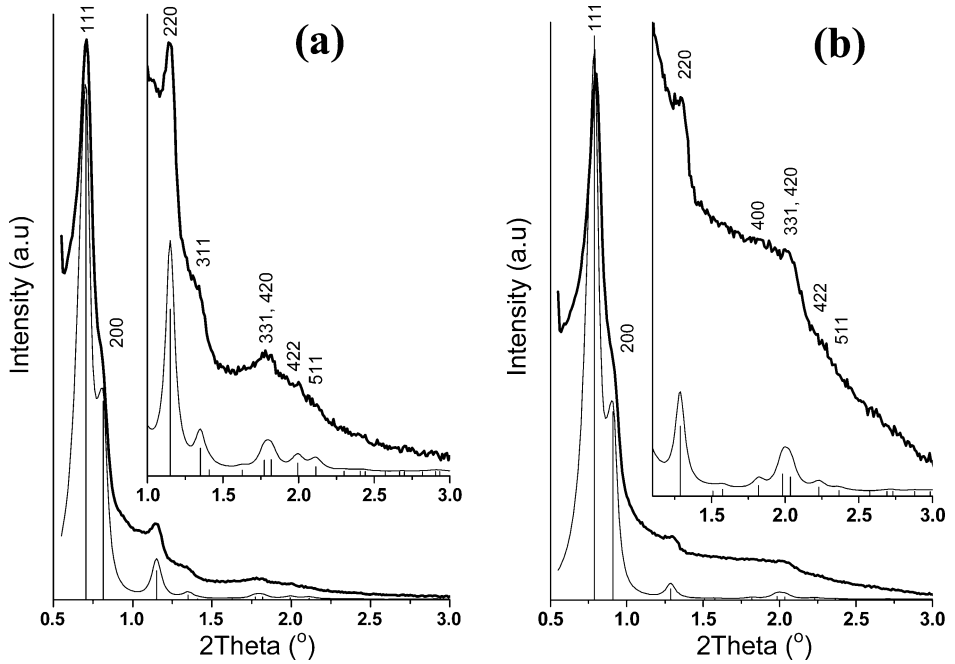

Figure 4. Experimental (solid line) and simulated (dashed line) X-ray powder diffraction profiles obtained for cubic *Fm*3*m* mesoporous silica samples measured on laboratory equipment: (a) AS-100 and (b) CA-100. The reflection positions are marked by drop lines.

between the experimental and calculated XRD profiles. As shown in Figures 3 and 4, the structure model provided full matching between the experimental and calculated XRD peak positions and intensities for both as-synthesized and calcined samples (see also Supporting Information, Figure S1). The final structure parameters obtained by the CDF modeling are listed in Table 1. It should be noted that the cavity diameters obtained by XRD modeling and physisorption data differ only by 0.4−1.0 nm, which is rather good consistency considering the simplified models used in XRD and physisorption calculations. The material synthesized at 45 °C has smaller cage diameter compared to the samples synthesized at higher temperatures. The fraction of cage volume per cubic unit cell in CA-45 is 0.11 (for the pore diameter of 6.5 nm from XRD) or 0.13 (for the pore diameter of 6.8 nm from the adsorption measurement), but for CA-100 this fraction is 0.18 (for the pore diameter of 8.5 nm from XRD) or 0.23 (for the pore diameter of 9.3 nm from adsorption). Thus, the reduced pore volume and surface area of CA-45 are related not to a partial structure collapse after calcination, but to the reduced cage diameter or, more precisely, to the reduced ratio of the cage volume to the volume of silica walls.

The excellent 3-D cubic mesoscopic order of KIT-5 is further confirmed by transmission electron microscopy. In Figures 5 and 6, characteristic TEM images of the materials are shown in comparison with respective TEM simulations. It should be noted that images taken along the [110] direction reveal no intergrowths with the 3-D hexagonal phase, which were often reported to occur for other cage-type mesoporous silicas (SBA-2, SBA-12, and FDU-1),[9,12,20] giving further evidence for the purity of this cubic *Fm*3*m* phase. The presence of the "twinned" hexagonal-close-packed structure can be ruled out, since the Fourier diffractograms corresponding to the images taken along [110] show no stacking faults and no streaking effects.[9,12] Contrary to the data presented by Fan et al.,[13] our TEM observations did not reveal (111) projections for the materials studied. The absence of (111) TEM projections with noticeable contrast is expectable for *Fm*3*m* close-packed cage mesostructures. TEM projections demonstrate noticeable contrast when

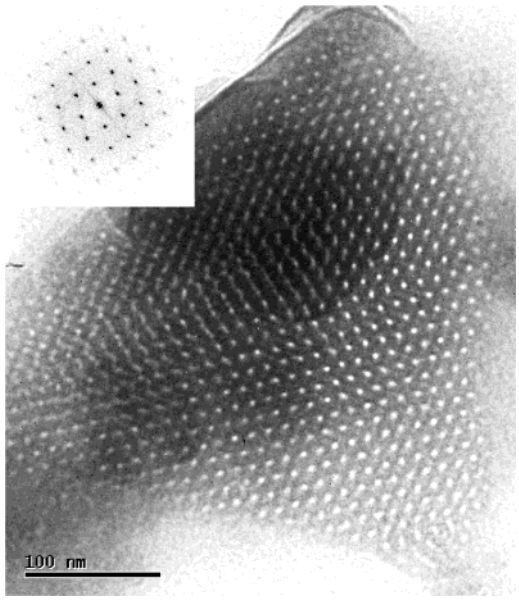

Figure 5. Transmission electron microscopy image of KIT-5 particle viewed from [110] direction. The inset shows the respective Fourier diffractogram.

they contain Fourier diffraction components corresponding to the most intense XRD reflections. For *Fm*3*m* close-packed cage materials, the characteristic TEM projections are (100), (110), and (211), since their Fourier diffractograms comprise (111)- and (200)-type reflections (Figure 6). Projection (111) for *Fm*3*m* lattice does not comprise (111) or (200) Fourier components; thus its observation by Fan et al.[13] may indicate that they dealt with a different type of mesostructure.

The use of hydrothermal treatment temperatures above 130 °C for a prolonged period provokes a marked evolution of the XRD pattern (Supporting Information, Figure S2), suggesting structural distortion or possible change of the symmetry that, however, requires further detailed investigations.

The 3-D cubic structure can be viewed as a compact cubic close packing of globular micellar aggregates surrounded by

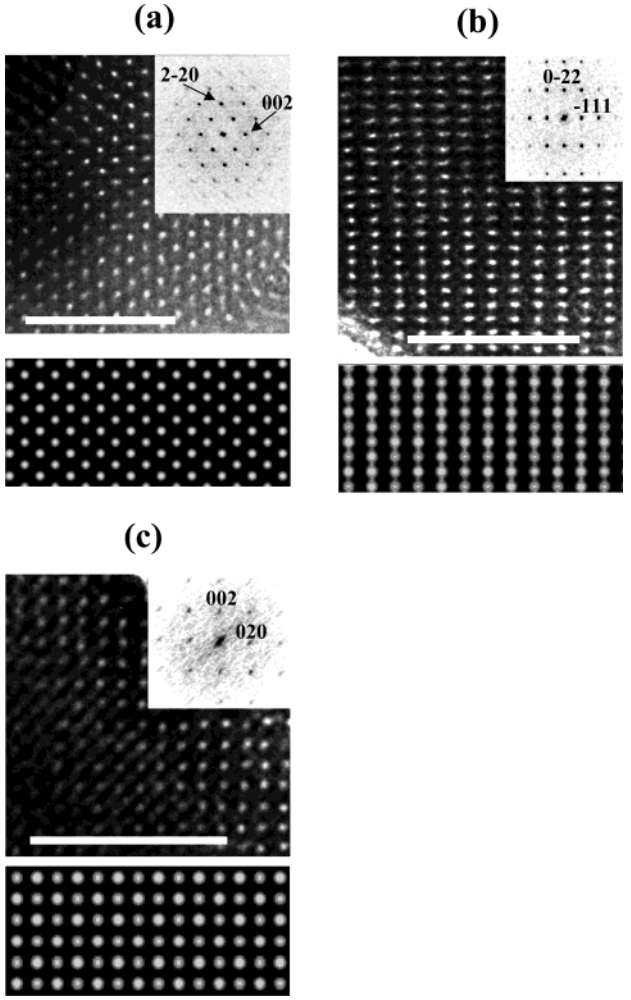

Figure 6. TEM images of KIT-5 (CA-100) taken along (a) [110], (b) [211], and (c) [100] incidences, and respective Fourier diffractograms. top: Experimental TEM images. bottom: Simulated TEM patterns. Scale bar, 100 nm.

thick silica walls, or cagelike pores after removal of the template. The aqueous synthesis route to achieve highly ordered cubic *Fm*3*m* mesoporous silica is based on the use of F127 triblock copolymer ($EO_{106}PO_{70}EO_{106}$), which exhibits high hydrophilic to hydrophobic volume ratio (high EO/PO) implying high curvature of the micelles, and TEOS as the silica precursor in dilute acidic conditions. We showed recently that the use of low HCl concentrations was critical in achieving precise control of the mesophase formation.[21] It was suggested that the dilute acidic regime allowed a more facile thermodynamic control of the mesostructured silica assembly instead of formation dominated by kinetic factors. The decrease in the mesophase formation kinetics by reducing the concentration of HCl is thought here to be appropriate for optimized cooperative assembly of highly curved micelles and silicates into well-ordered close-packed cubic structures.

Conclusions

In conclusion, we have developed an aqueous synthesis method to prepare highly ordered large-cage mesoporous silica with cubic *Fm*3*m* close-packed structure, based on the use of TEOS with $EO_{106}PO_{70}EO_{106}$ triblock copolymer (F127) at low HCl concentrations. The structure assignment to *Fm*3*m* symmetry was established by modeling XRD and TEM that are fully consistent with the experimental data. We confirmed that simple application of hydrothermal treatments at various temperatures ranging from 45 to 150 °C enables an effective tailoring of the mesopore diameters and apertures. Above 130 °C, however, marked structural changes accompanying the opening of the pore entrances are observed. Further, the use of experimental and simulated X-ray diffraction patterns and TEM images is shown to be particularly powerful to elucidate the symmetry and structure of ordered mesoporous materials, and this methodology might, therefore, be more systematically employed in the future to prevent erroneous speculations. We expect the synthesis route described here to generate various fundamental studies such as comprehensive structure characterization using X-ray and electron crystallography, and modeling of the adsorption phenomena in spherical mesopores, in addition to encasing of guest species, surface modification of the pore walls, and other various advanced applications.

Acknowledgment. This work was supported by the Creative Research Initiative Program of the Korean Ministry of Science and Technology, the School of Molecular Science through the Brain Korea Project, and Grants INTAS 01-2283, KRSF-RFBR 02-03-97704, and RFBR 03-03032127.

Supporting Information Available: Figures S1 and S2 showing XRD profiles for samples AS-45, CA-45, and CA-150(48 h). This material is available free of charge via the Internet at http://pubs.acs.org.

References and Notes

(1) For reviews and recent developments see: (a) Ying, J. Y.; Mehnert, C. P.; Wong, M. S. *Angew. Chem., Int. Ed.* **1999**, *38*, 56. (b) Schüth, F. *Chem. Mater.* **2001**, *13*, 3184. (c) Schmidt, W.; Schüth, F. *Adv. Mater.* **2002**, *14*, 629. (d) Stein, A. *Adv. Mater.* **2003**, *15*, 763.

(2) Zhao, D.; Huo, Q.; Feng, J.; Chmelka, B. F.; Stucky, G. D. *J. Am. Chem. Soc.* **1998**, *120*, 6024.

(3) Sakamoto, Y.; Kaneda, M.; Terasaki, O.; Zhao, D.; Kim, J. M.; Stucky, G. D.; Shin, H. J.; Ryoo, R. *Nature* **2000**, *408*, 449.

(4) Kim, S.-S.; Pauly, T. R.; Pinnavaia, T. J. *Chem. Commun.* **2000**, 1661.

(5) Yu, C.; Yu, Y.; Zhao, D. *Chem. Commun.* **2000**, 575.

(6) Kipkemboi, P.; Fogden, A.; Alfredsson, V.; Flodström, K. *Langmuir* **2001**, *17*, 5398.

(7) Van der Voort, P.; Benjelloun, M.; Vansant, E. F. *J. Phys. Chem. B* **2002**, *106*, 9027.

(8) Flodström, K.; Alfredsson, V. *Microporous Mesoporous Mater.* **2003**, *59*, 167.

(9) Matos, J. R.; Kruk, M.; Mercuri, L. P.; Jaroniec, M.; Zhao, L.; Kamiyama, T.; Terasaki, O.; Pinnavaia, T. J.; Liu, Y. *J. Am. Chem. Soc.* **2003**, *125*, 821.

(10) Flodström, K.; Alfredsson, V.; Källrot, N. *J. Am. Chem. Soc.* **2003**, *125*, 4402.

(11) Kleitz, F.; Choi, S. H.; Ryoo, R. *Chem. Commun.* **2003**, 2136.

(12) Sakamoto, Y.; Díaz, I.; Terasaki, O.; Zhao, D.; Pérez-Pariente, J.; Kim, J. M.; Stucky, G. D. *J. Phys. Chem. B* **2002**, *106*, 3118.

(13) Fan, J. F.; Yu, C.; Gao, F.; Lei, J.; Tian, B.; Wang, L.; Luo, Q.; Tu, B.; Zhou, W.; Zhao, D. *Angew. Chem., Int. Ed.* **2003**, *42*, 3146.

(14) Solovyov, L. A.; Kirik, S. D.; Shmakov, A. N.; Romannikov, V. N. *Microporous Mesoporous Mater.* **2001**, *44*−*45*, 17.

(15) Rietveld, H. M. *J. Appl. Crystallogr.* **1969**, *2*, 65.

(16) (a) Ravikovitch, P. I.; Neimark, A. V. *Langmuir* **2002**, *18*, 1550. (b) Ravikovitch, P. I.; Neimark, A. V. *Langmuir* **2002**, *18*, 9830.

(17) Barrett, E. P.; Joyner, L. G.; Halenda, P. P. *J. Am. Chem. Soc.* **1951**, *73*, 373.

(18) Groen, J. C.; Peffer, L. A. A.; Pérez-Ramírez, J. *Microporous Mesoporous Mater.* **2003**, *60*, 1.

(19) Kruk, M.; Jaroniec, M. *Chem. Mater.* **2003**, *15*, 2942.

(20) Zhou, W.; Hunter, H. M. A.; Wright, P. A.; Ge, Q.; Thomas, J. M. *J. Phys. Chem. B* **1998**, *102*, 6934.

(21) Choi, M.; Heo, W.; Kleitz, F.; Ryoo, R. *Chem. Commun.* **2003**, 1340.